I. Adiabatic Invariants and Magnetospheric Models

I.1 Preliminary Considerations

As long as it remains trapped within the earth's magnetosphere, a radiation-belt particle of mass m and charge q typically executes a hierarchy of three distinct forms of quasi-periodic motion. The most rapid of these is *gyration* about a field line at frequency $\Omega_1/2\pi = -qB/2\pi mc$, where $\mathbf{B}$ is the local magnetic-field intensity and c is the speed of light. The instantaneous center of the gyration orbit is known as the particle's *guiding center*. An average over gyration reveals an oscillation of the guiding center between magnetic *mirror points*, which are located at a pair of well-defined positions along a path that very nearly coincides with the original field line. This periodic *bounce motion* between mirror points proceeds at a frequency $\Omega_2/2\pi \sim v/2\pi S$, where v is the speed of the particle and S is the arc length of the entire field line. Finally, an average over the bounce motion reveals an *azimuthal drift* of the guiding-center trajectory. This drift motion generates a shell encircling the earth; complete circuits of this shell are accomplished at the drift frequency $\Omega_3/2\pi \sim \langle v^2/2\pi\Omega_1 S^2\rangle$, where the angle brackets denote an average over the entire particle orbit.

The time scales for gyration, bounce, and drift are respectively separated by a factor of order $\varepsilon \equiv \langle v/\Omega_1 S\rangle$. The limit $|\varepsilon| \ll 1$ is required for performing the averages mentioned above so as to separate the motion into the three distinct components. This condition imposes the requirement that the gyroradius be much smaller everywhere than the length of the guiding field line. Radiation-belt particles of interest here are thus distinguished by the requirement $|\varepsilon| \ll 1$ from very energetic particles such as galactic cosmic rays, which may have gyroradii as large as the magnetosphere. This limitation on radiation-belt energies is not a universally accepted convention, but it is conceptually useful to restrict the radiation belts to particles whose kinematics fall within the hierarchy outlined above. Special methods of numerical analysis [17] beyond the scope of the present treatment must generally be employed where $|\varepsilon| \gtrsim 1$. Such methods trace the details of each particle trajectory.

The limits on particle energy appropriate to the radiation belts can be estimated by calculating ε for a special class of particles, *viz.*, the class of particles magnetically confined to the equatorial plane

of a dipole field. These particles can be thought of as "mirroring at the equator", or as bouncing with infinitesimal amplitude but finite frequency. If a is the radius of the earth (in which the magnetic dipole is assumed to be centered), the length of a field line that crosses the equatorial plane at a distance of L earth radii from the center is given (see Section I.4) by

$$S = 2La[1 + 1/2\sqrt{3}) \ln(2 + \sqrt{3})] \approx 2.7603\, La. \tag{1.01}$$

For a particle carrying the charge of Z protons, it follows that

$$\varepsilon \approx \beta L^2 (mc^2/2.76\, qB_0 a) \approx \beta L^2 (mc^2/216\, Z\,\mathrm{GeV}), \tag{1.02}$$

where $\beta = v/c$, c is the speed of light, and B_0 (≈ 0.31 gauss) is the equatorial magnetic-field intensity at the earth's surface. The limit $|\varepsilon| \ll 1$ required of radiation-belt particles is therefore satisfied by kinetic energies up to approximately $10/L^2$ GeV for protons, alpha particles, and other light ions, as well as relativistic electrons.

I.2 Action-Angle Variables

The three distinct periodicities associated with gyration, bounce, and drift motion give rise to a hierarchy consisting of three pairs of action-angle variables. The action variables J_i ($i = 1,2,3$) are canonically defined [7] by the path integrals

$$J_i = \oint_i [\mathbf{p} + (q/c)\mathbf{A}] \cdot d\mathbf{l}, \tag{1.03}$$

where $\mathbf{p}$ is the particle momentum and $\mathbf{A}$ is the electromagnetic vector potential. The first action integral J_1 corresponds to gyration about a field line. The first term of (1.03) for $i = 1$ is therefore equal to $2\pi p_\perp^2/m|\Omega_1|$, where $p_\perp$ is the component of $\mathbf{p}$ normal to $\mathbf{B}$. This follows from the fact that the orbit of gyration has a circumference equal to $2\pi v_\perp/|\Omega_1|$, where $v_\perp = p_\perp/m$. The second term of (1.03) for $i = 1$ is equal to q/c times the magnetic flux enclosed by the orbit of gyration. The net result is that

$$J_1 = \pi p_\perp^2 c/B|q| \tag{1.04}$$

if one observes the sign convention that Ω_1 is positive for electrons, which gyrate in a positive (counterclockwise) sense about the field line. Since the rest mass m_0 is a constant of the motion, it is usual to extract from (1.04) a quantity

$$M \equiv p_\perp^2/2m_0 B, \tag{1.05}$$

known as the *first adiabatic invariant*. This is not empty nomenclature, for M is indeed an invariant of the motion if the fields (*e.g.*, magnetic, electric, gravitational) seen by the particle remain virtually constant in time over the entire orbit of gyration. In practice this requires also that such fields do not vary significantly on a spatial scale as small as $v_\perp/|\Omega_1|$. Note that M/γ is equal to the magnetic moment of the particle, where γ $(=m/m_0)$ is the usual relativistic factor.

The second action integral J_2 is evaluated along the bounce path, which is essentially parallel to the guiding field line and therefore encloses no magnetic flux. Convention does not distinguish between the second action integral J_2 and the *second adiabatic invariant*

$$J \equiv J_2 = \oint p_{||} ds, \tag{1.06}$$

where $p_{||}$ is the component of $\mathbf{p}$ parallel to $\mathbf{B}$ and s is a curvilinear coordinate that measures distance along a field line from the equator. The adiabatic invariance of J holds for a particle acted upon by forces that remain virtually constant in time over the bounce period.

The third action integral J_3 is associated with the azimuthal drift motion. The integral around the drift shell may be evaluated along any closed curve that lies entirely on this surface and encircles the earth. For this action integral the first term of (1.03) is of order ε^2 (and therefore negligible) compared to the second. It follows that

$$J_3 = (q/c)\Phi, \tag{1.07}$$

where Φ, the magnetic flux enclosed by the drift shell, is known as the *third adiabatic invariant*. The integral is independent of the path within the limitations specified above because no field lines intersect the drift shell in the limit $|\varepsilon| \ll 1$. The sign convention adopted in (1.07) corresponds to that for Ω_1, since the *drift* of electrons is also counterclockwise. Thus, the signature of Φ is positive for $q>0$ and negative for $q<0$. The third invariant is generally conserved for a particle acted upon by forces that remain virtually constant in time over the complete drift period. Figure 6 provides contour plots of the gyration, bounce, and drift frequencies versus kinetic energy and L for protons and electrons mirroring at the equator of a geomagnetic dipole field [see Section I.4].

By their execution of all three types of adiabatic motion, particles that belong to the radiation belts are distinguished from a variety of other particles found within the magnetosphere. Thus, solar cosmic-ray particles having energies appropriate to the radiation belts often enter the geomagnetic tail and descend to the polar caps. Since the tail does not support bounce motion, however, these particles must either precipitate into the polar atmosphere or mirror magnetically and return

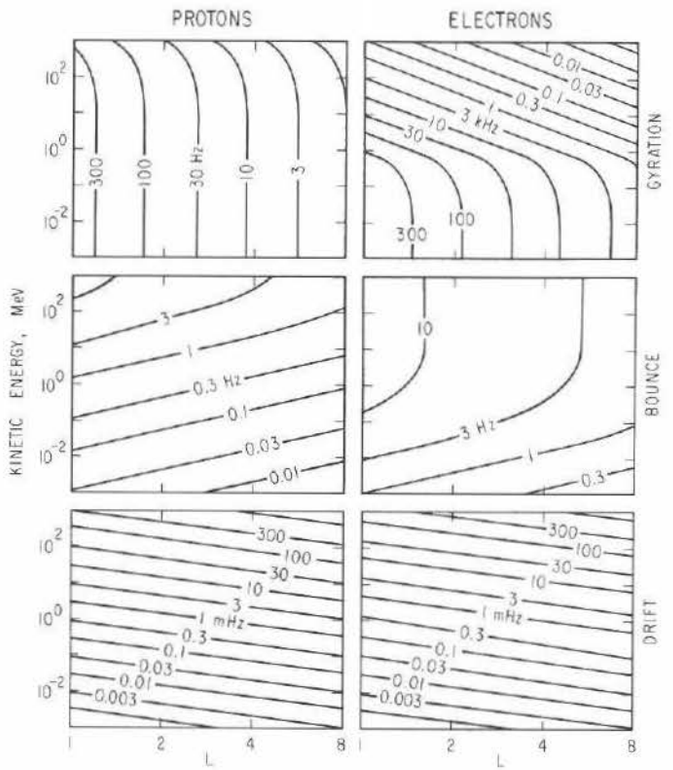

Fig. 6. Contours of constant adiabatic gyration, bounce, and drift frequency for equatorially mirroring particles in a dipole field. Adiabatic approximation fails in upper right-hand corners ($E \sim 1$ GeV, $L \sim 8$), since $\Omega_1 \sim \Omega_2 \sim \Omega_3$ implies $|\varepsilon| \sim 1$.

to interplanetary space. As they do not remain trapped within the magnetosphere, these particles disappear from the polar caps as soon as their immediate source (*e.g.*, a solar flare) is extinguished.

Particles that populate the quasi-trapping regions (see Introduction) are similarly excluded from the radiation belts by their inability to complete a drift period. A quasi-trapping region supports bounce motion and yields a well-defined second invariant, but it generates only partial drift shells that intersect the magnetospheric surface either at the magnetopause or at the neutral sheet. Thus, particles whose mirror points lie within a quasi-trapping region do not persist after withdrawal of their source and (by this convention) do not belong to the radiation belts.

For those particles that do execute all three types of quasi-periodic motion, the quantities $J_i/2\pi$ ($i=1,2,3$) constitute a complete set of canonical angular momenta. The angular coordinates to which the $J_i/2\pi$ are conjugate can be identified as the phases φ_i that describe the progress made by a particle toward the completion of a gyration, bounce period, and drift period. Each phase φ_i is considered to advance at its own characteristic rate Ω_i, so as to achieve an increment of 2π upon completion of the period $2\pi/\Omega_i$ of the motion.

Conservation of the adiabatic invariants M, J, and Φ requires, in effect, that φ_1, φ_2, and φ_3 be cyclic coordinates [7] of the dynamical problem. Violation of the invariants occurs only in the presence of forces that vary on a sufficiently short spatial or temporal scale that particles having different phases respond differently. This, of course, is the underlying reason for the validity of adiabatic theory as a kinematical foundation for the study of radiation-belt dynamics.

I.3 Liouville's Theorem

The kinematical state of a particle in three-dimensional motion can, in general, be defined instantaneously by specifying its three coordinates of position and three components of canonical momentum. These six quantitites locate a point in the six-dimensional continuum known as *phase space*. As time evolves, the motion of the particle generates a trajectory in phase space.

A system consisting of N distinct particles of a given species (*e.g.*, protons) is described by a set of N distinct points in phase space. When N is very large, it proves convenient to describe the distribution of these points in phase space by means of a six-dimensional density function $f(\pi_i,q_i;t)$ where the π_i ($i=1,2,3$) are components of canonical momentum, the q_i are coordinates of position, and t is the time. This distribution function has the usual significance that $f d^3\pi\ d^3\mathbf{q}$ is the number of particles instantaneously occupying the six-dimensional volume $d^3\boldsymbol{\pi}\ d^3\mathbf{q}$ in canonical phase space.

In Hamiltonian mechanics the temporal evolution of $f(\pi_i,q_i;t)$ is specified by Liouville's theorem [7], which asserts that

$$(df/dt)\equiv(\partial f/\partial t)+\sum_{i=1}^{3}\left[\dot{\pi}_i(\partial f/\partial \pi_i)+\dot{q}_i(\partial f/\partial q_i)\right]=0 \tag{1.08}$$

along any dynamical trajectory in phase space. In more picturesque terms, the phase-space volume containing the system of N distinct representative points moves incompressibly through phase space. The

dynamical trajectory of an individual particle is governed by the equations

$$\dot{\pi}_i=-\partial H/\partial q_i \tag{1.09a}$$

$$\dot{q}_i=\partial H/\partial \pi_i, \tag{1.09b}$$

where $H(\pi_i,q_i;t)$ is the Hamiltonian. Liouville's theorem implies that the content of an infinitesimal six-dimensional volume $d^3\pi\ d^3\mathbf{q}$ surrounding a particle's location in phase space remains invariant as the particle executes its dynamical trajectory. This means that a unit Jacobian characterizes the transformation of such an infinitesimal volume moving in accordance with the laws of classical mechanics. Indeed, the execution of a dynamical trajectory is describable by a sequence of infinitesimal contact transformations [7]. Each of these infinitesimal transformations has the properties that

$$\pi_i\rightarrow\pi_i+d\pi_i=\pi_i-(\partial H/\partial q_i)dt \tag{1.10a}$$

$$q_i\rightarrow q_i+dq_i=q_i+(\partial H/\partial \pi_i)dt \tag{1.10b}$$

$$H\rightarrow H+dH=H+(\partial H/\partial t)dt \tag{1.10c}$$

in accordance with (1.09).

Apart from its utility in specifying the adiabatically invariant action integrals J_i, the canonical momentum $\boldsymbol{\pi}$ is not a convenient physical quantity in the study of radiation-belt dynamics. It is far more convenient to deal with the locally observable particle momentum $\mathbf{p}$ alone than in combination with $(q/c)\mathbf{A}$, since the electromagnetic vector potential $\mathbf{A}$ is neither locally observable nor uniquely defined. Accordingly, it becomes advantageous at this point to introduce the distribution function $f(\mathbf{p},\mathbf{r};t)$, which represents the density of particles in a six-dimensional (but non-canonical) position-momentum space. The relation between $f(\mathbf{p},\mathbf{r};t)$ and $f(\boldsymbol{\pi},\mathbf{q};t)$ is readily obtained via the algebraic transformation

$$\boldsymbol{\pi}=\mathbf{p}+(q/c)\mathbf{A} \tag{1.11a}$$

$$\mathbf{q}=\mathbf{r}. \tag{1.11b}$$

No loss of generality is suffered by supposing that the coordinates are Cartesian. In this case it is easy to verify that the transformation defined by (1.11) has a unit Jacobian, from which it follows that $f(\mathbf{p},\mathbf{r};t)=f(\boldsymbol{\pi},\mathbf{q};t)$. The distribution function $f(\mathbf{p},\mathbf{r};t)$, of course, has the significance that $f d^3\mathbf{p}\ d^3\mathbf{r}$ is the number of particles instantaneously occupying the infinitesimal six-dimensional volume $d^3\mathbf{p}\,d^3\mathbf{r}$ in position-momentum space. Since $f(\mathbf{p},\mathbf{r};t)$ is numerically equal to the phase-space density $f(\boldsymbol{\pi},\mathbf{q};t)$, it follows that f remains constant along a dynamical trajectory in position-momentum space. This property is summarized

by the equation (known as the Vlasov equation)

$$(\partial f/\partial t)+(\mathbf{p}/m)\cdot(\partial f/\partial \mathbf{r})+\mathbf{F}\cdot(\partial f/\partial \mathbf{p})=0, \tag{1.12}$$

where $\mathbf{F}=\dot{\mathbf{p}}$ is the force applied to a particle of momentum $\mathbf{p}$ located at position $\mathbf{r}$. The particle velocity $\mathbf{v}$ is equal to $\mathbf{p}/m$, and the relativistic mass m exceeds the rest mass m_0 by the factor

$$\gamma=[1+(p/m_0c)^2]^{1/2}, \tag{1.13}$$

where c is the speed of light.

The Vlasov equation is sometimes cast in the alternative form [18]

$$(\partial f/\partial t)+\sum_i v_i(\partial f/\partial r_i)+\sum_{ij}(F_i/m)[\delta_{ij}-(v_iv_j/c^2)](\partial f/\partial v_j)=0, \tag{1.14}$$

where δ_{ij} is the Kronecker symbol ($=1$ for $i=j$ and $=0$ for $i\neq j$). This form can be derived from (1.12) by noting that

$$m(\partial v_j/\partial p_i)=\delta_{ij}-(v_iv_j/c^2). \tag{1.15}$$

As formulated here, the Vlasov equation takes account of the relativistic kinematics of charged particles but does not include certain processes (such as collisions) that are not easily described by a Hamiltonian. Such processes are best added phenomenologically to the Vlasov description.

I.4 The Dipole Field

For purposes of analytical calculation it is often convenient to represent the geomagnetic field as the field of a magnetic dipole centered within a perfectly spherical earth. The dipole axis is assumed to be coincident with the axis of rotation, and the spherical polar coordinates r, θ, and φ are measured from the center of the earth, the north pole, and the midnight meridian, respectively. The field intensity is given by

$$\mathbf{B}=-B_0(2\hat{\mathbf{r}}\cos\theta+\hat{\boldsymbol{\theta}}\sin\theta)(a/r)^3, \tag{1.16}$$

where a is the radius of the earth and $B_0(\approx 0.31$ gauss) is the equatorial ($\theta=\pi/2$) magnitude of $\mathbf{B}$ at $r=a$. A field line that intersects the equatorial plane at a distance $r=La$ from the origin generates a drift shell to which is assigned the dimensionless parameter L. The differential equation of this field line is

$$dr/d\theta=rB_r/B_\theta=2r\operatorname{ctn}\theta, \tag{1.17a}$$

from which it is deduced that

$$r=La\sin^2\theta. \tag{1.17b}$$

The element of arc length along the field line is therefore

$$ds=La(1+3\cos^2\theta)^{1/2}\sin\theta\,d\theta, \tag{1.18}$$

and from this expression follows the value given by (1.01) for the total length S of the field line.

In the formal theory of adiabatic motion it is customary to introduce the Euler potentials α and β such that $\mathbf{A}=\alpha\nabla\beta$ and (therefore) $\mathbf{B}=\nabla\alpha\times\nabla\beta$. The dipole field can be generated by assigning the Euler potentials $\alpha=-B_0a^2/L$ and $\beta=\varphi$, so that

$$\mathbf{A}=-B_0\hat{\boldsymbol{\varphi}}(a^3/r^2)\sin\theta. \tag{1.19}$$

These assignments are not unique, since they can be modified by a gauge transformation without altering any physical consequences. The chosen representations, however, have the special significance that $|\Phi|=-2\pi\alpha$ and $\varphi_3=\beta$, *i.e.*, the Euler potentials are immediately related to the third invariant and drift phase, respectively. Euler potentials are used elsewhere in describing the geomagnetic field [19], but are omitted from further discussion in this volume.

The kinematical description of the radiation belts is simplified greatly by the customary assumption that field lines are equipotential. Of course, this assumption is not rigorously justified, but for particles of sufficiently large energy the variations of time-independent electrostatic and gravitational potentials along a field line are unimportant[4].

The adiabatic motion of a charged particle influenced only by a magnetostatic field of mirror geometry conserves both M, as given by (1.05), and the kinetic energy $E=m_0c^2(\gamma-1)$. It follows from (1.13), then, that $p^2(\equiv p_\perp^2+p_\parallel^2)$ remains constant, where $p_\parallel$ is the component of momentum parallel to $\mathbf{B}$. This component of $\mathbf{p}$ vanishes at each mirror point, where the guiding-center magnetic-field intensity is denoted B_m. Here the angle between $\mathbf{p}$ and $\mathbf{B}$, known as the *pitch angle*, is 90°. The minimum angle between $\mathbf{p}$ and $\mathbf{B}$ attained during the bounce period is known as the *equatorial pitch angle*, because this minimum occurs at that point along the guiding field line at which B is a minimum; in the dipole field this point lies on the equatorial plane.

The bounce motion of a particle's guiding center along an equipotential field line has a period

$$2\pi/\Omega_2=(m/p)\oint[1-(B/B_m)]^{-1/2}ds, \tag{1.20}$$

[4]Gravity is totally negligible for particle energies $\gtrsim 1$ keV. Electrostatic-potential variations along a field line in the radiation zone may amount to 10—100 volts, and so are similarly negligible for particle energies $\gtrsim 1$ keV [11].

where the integral is evaluated along the guiding field line. Both p and M are constants of the bounce motion, and the integral above can be interpreted either as twice the *spiral* path length between mirror points along the actual trajectory, or as the integral of the pitch-angle secant along the guiding-center trajectory. The instantaneous value of $\dot{s}$, in other words, is given by

$$p_{\parallel}/m=[(p/m)^2-(2m_0MB/m^2)]^{1/2}=(p/m)[1-(B/B_m)]^{1/2}. \quad (1.21)$$

The maximum value of $p_{\parallel}$ along the bounce path corresponds to the minimum of B. Thus, if x is the cosine of the equatorial pitch angle and B_e is the equatorial guiding-center field magnitude, it follows that

$$x^2=1-(B_e/B_m)=1-y^2, \quad (1.22)$$

where y is the sine of the equatorial pitch angle.

For the dipole field it follows from (1.16) and (1.17 b) that $B_e=B_0L^{-3}$ and that

$$B=(B_0/L^3)(1+3\cos^2\theta)^{1/2}\csc^6\theta. \quad (1.23)$$

The bounce period $2\pi/\Omega_2$ is therefore representable as

$$2\pi/\Omega_2=(4mLa/p)T(y), \quad (1.24a)$$

where

$$T(y)=\int_{\theta_m}^{\pi/2}\frac{\sin\theta(1+3\cos^2\theta)^{1/2}\,d\theta}{[1-y^2\csc^6\theta(1+3\cos^2\theta)^{1/2}]^{1/2}}. \quad (1.24b)$$

The colatitude θ_m of the northern mirror point is given by the relation

$$y=(1+3\cos^2\theta_m)^{-1/4}\sin^3\theta_m. \quad (1.25)$$

At $y=0$ the integral for $T(y)$ is easily evaluated. The result is $T(0)=S/2La$, where S (the length of the field line) is given by (1.01). At $y=1$ ($\theta_m=\pi/2$) the integral can be evaluated by an appeal to the theory of small-amplitude oscillations [7] about the equator. The equation of motion for such a particle subjected to magnetostatic forces is

$$m\ddot{s}=-(M/\gamma)(\partial B/\partial s)=-(p^2/2mB_e)(\partial^2B/\partial s^2)_e s, \quad (1.26)$$

where the subscript e denotes the equator ($s=0$). The magnetic moment in general is equal to M/γ, and this amounts to $p^2/2mB_e$ for an equatorially mirroring particle. The equatorial value of $\partial^2B/\partial s^2$ is given by

$$(\partial^2B/\partial s^2)_e=\hat{\mathbf{B}}_e\cdot\nabla(\hat{\mathbf{B}}\cdot\nabla B)_e=(3/La)^2B_e, \quad (1.27)$$

so that $\Omega_2=(p/m)(3/\sqrt{2}\,La)$. It follows that $T(1)=(\pi/6)\sqrt{2}$.

For $0<y<1$, exact evaluation of (1.24b) in terms of elementary functions of y is impossible. A very good estimate, however, is provided by the formula [20]

$$T(y)\approx T(0)-\tfrac{1}{2}[T(0)-T(1)](y+y^{1/2}), \quad (1.28a)$$

where

$$T(0)=1+(1/2\sqrt{3})\ln(2+\sqrt{3})\approx 1.3802 \quad (1.28b)$$

$$T(1)=(\pi/6)\sqrt{2}\approx 0.7405 \quad (1.28c)$$

$$\tfrac{1}{2}[T(0)-T(1)]\approx 0.3198; \quad (1.28d)$$

at worst, this estimate deviates from the numerically computed function $T(y)$ by less than 1% (see Table 1).

Table 1. Functions of Bounce Motion in Dipole Field

θ_m	$y^{1/2}$	$\sin^{-1}y$	Exact T	Approx T	Exact Y	Approx Y
0°	0.00000	0.00°	1.380	1.380	2.760	2.760
1°	0.00194	0.00°	1.380	1.380	2.760	2.758
5°	0.02165	0.03°	1.376	1.373	2.741	2.730
10°	0.06102	0.21°	1.366	1.359	2.682	2.6633
15°	0.1114	0.71°	1.350	1.341	2.587	2.565
20°	0.1701	1.66°	1.327	1.316	2.457	2.434
25°	0.2352	3.17°	1.298	1.287	2.296	2.275
30°	0.3051	5.34°	1.264	1.253	2.109	2.091
35°	0.3785	8.23°	1.224	1.213	1.901	1.886
40°	0.4539	11.89°	1.179	1.169	1.678	1.666
45°	0.5303	16.33°	1.129	1.121	1.446	1.437
50°	0.6062	21.56°	1.076	1.069	1.211	1.205
55°	0.6804	27.58°	1.020	1.014	0.9793	0.9761
60°	0.7515	34.38°	0.963	0.959	0.7577	0.7562
65°	0.8178	41.97°	0.906	0.905	0.5521	0.5517
70°	0.8773	50.32°	0.854	0.853	0.3693	0.3692
74°	0.9186	57.54°	0.816	0.816	0.2438	0.2438
78°	0.9528	65.20°	0.784	0.785	0.1408	0.1408
82°	0.9785	73.23°	0.760	0.761	0.06386	0.06387
86°	0.9945	81.54°	0.745	0.746	0.01617	0.01617
90°	1.0000	90.00°	0.740	0.740	0.00000	0.00000

The second invariant J, as given by (1.06), can be approximated by means of a formula derivable from (1.28). The invariant is given by

$$J=2pLaY(y), \quad (1.29a)$$

where

$$Y(y)=2\int_{\theta_m}^{\pi/2}\frac{\sin\theta(1+3\cos^2\theta)^{1/2}\,d\theta}{[1-y^2\csc^6\theta(1+3\cos^2\theta)^{1/2}]^{-1/2}}. \tag{1.29b}$$

The observation that

$$\frac{d}{dy}\left(\frac{Y}{y}\right)=-\frac{2T}{y^2} \tag{1.30}$$

enables $Y(y)$ to be estimated from (2.28). Since $Y(1)=0$, it follows that

$$Y(y)=2y\int_y^1 u^{-2}T(u)\,du\approx 2(1-y)T(0)+[T(0)-T(1)](y\ln y+2y-2y^{1/2}). \tag{1.31}$$

This estimate remains within 1% of the numerically computed $Y(y)$ for all values of y between 0 and 1 (see Table 1). Moreover, the exact analytical result that $Y(0)=2T(0)$ is reproduced by (1.31). An expansion for $x^2\equiv 1-y^2\ll 1$ reproduces the harmonic-oscillator approximation, which implies that

$$J=\oint p_{\|}\,ds=\oint(p_{\|}^2/m)\,dt\approx(p^2x^2/2m)(2\pi/\Omega_2) \tag{1.32a}$$

or

$$Y(y)\approx T(1)x^2=(\pi/6)\sqrt{2}\,x^2\approx 0.7405(1-y^2). \tag{1.32b}$$

In (1.32a) the time-averaged value of $p_{\|}^2$ is equal to half the maximum value, since $p_{\|}$ is a harmonically varying quantity in the limit of vanishing bounce amplitude. This maximum value, attained at the equator, is p^2x^2.

As a further application of (1.28) it is possible to estimate the pitch-angle dependence of the azimuthal drift frequency $\Omega_3/2\pi$. According to the sign convention introduced above, the drift phase φ_3 is a temporally increasing quantity, so that $\dot{\varphi}_3=-(q/|q|)\Omega_3$, where $\Omega_3=\dot{\varphi}$ is the time derivative of the particle's azimuthal coordinate (see Sections I.1 and I.2). It follows from Hamilton-Jacobi theory [7] that

$$\Omega_3=-(2\pi q/|q|)(\partial H/\partial J_3)_{M,J} \tag{1.33}$$

where H $(=\gamma m_0c^2)$ is the Hamiltonian. Evaluation of this expression is facilitated by noting that (1.13) implies $dH/dp=p/m$, while (1.07) implies $J_3=|q|(2\pi B_0a^2/cL)$. It follows from (1.05), (1.29), and (1.30) that

$$(\partial\ln y/\partial\ln L)_{M,J}=-Y/4T \tag{1.34a}$$

and

$$(\partial p/\partial L)_{M,J}=(p/4LT)(Y-6T)\equiv-[3p/LT(y)]D(y), \tag{1.34b}$$

where

$$12D(y)=6T(y)-Y(y). \tag{1.34c}$$

Simple algebraic manipulations thus lead to the formula

$$\begin{aligned}\Omega_3/2\pi&=-(3\gamma L/2\pi)(p/ma)^2(m_0c/qB_0)[D(y)/T(y)]\\&=-(3L/2\pi\gamma)(\gamma^2-1)(c/a)^2(m_0c/qB_0)[D(y)/T(y)]\end{aligned} \tag{1.35}$$

for the azimuthal drift frequency.

Since $Y(1)=0$ and $Y(0)=2T(0)$, it follows at once that $T(1)=2D(1)$ and $T(0)=3D(0)$. For intermediate values of y, an accurate analytical approximation to $D(y)$ is provided by (1.28) and (1.31). Explicitly stated, the result is

$$12D(y)\approx 4T(0)-[3T(0)-5T(1)]y-[T(0)-T(1)](y\ln y+y^{1/2}). \tag{1.36}$$

The estimate for $D(y)/T(y)$ provided by (1.28) and (1.36) deviates at

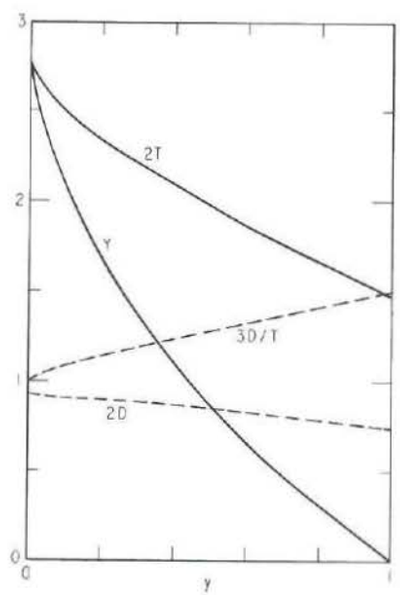

Fig. 7. Functions governing the pitch-angle dependence of bounce and drift frequencies in a dipole field.

worst by less than 0.2% from the numerically computed ratio $D(y)/T(y)$. Figure 7 indicates graphically the dependence of $T(y)$, $Y(y)$, $D(y)$, and $D(y)/T(y)$ upon y. The functions $D(y)$ and $T(y)$ and their ratio all vary monotonically with y in such a manner that, for a given particle species and energy, the bounce frequency and drift frequency are maximal for particles that mirror at the equator and progressively smaller for particles having mirror points at progressively higher (poleward) latitudes. This variation of bounce and drift frequency with equatorial pitch angle ($\sin^{-1} y$), however, is remarkably weak, as it amounts to less than a factor of two in each case.

The equations of this section summarize the adiabatic motion of a particle trapped in the field of a magnetic dipole centered within the earth. The three invariants M, J, and Φ are conserved, and (since the field is symmetric in azimuth) the drift shell is generated by rotating the guiding field line about the dipole axis. The gyrofrequency $\Omega_1/2\pi$ varies with the instantaneous position of the guiding center along the field line. The minimum magnitude of Ω_1 is given by $|q|B_0/mcL^3$ and is attained at the equator. The maximum value is $|q|B_0/mcL^3y^2$ and is attained at the mirror latitude. Since the drift shell is symmetric about the dipole axis, the bounce frequency $\Omega_2/2\pi$ is independent of azimuth and given by $\Omega_2/2\pi=[p/4mLaT(y)]$. A further consequence of azimuthal symmetry is that the bounce-averaged azimuthal coordinate φ advances eastward (in the case of a negatively charged particle) or retreats westward (for a positive ion) at a constant rate equal to the value of Ω_3 given by (1.35). The functional forms of $T(y)$, $Y(y)$, and $D(y)$ noted above are, of course, valid only for the dipole field.

I.5 The Distorted Field

The centered-dipole field is only a gross idealization of the true geomagnetic field. The idealized field has value as a standard of reference for the analysis of radiation-belt dynamics, however, and this value is enhanced by an appreciation of the extent to which the true field deviates from the ideal.

The dipolar component of the earth's field originates in the molten core. Higher multipoles of the core field diminish in intensity by comparison with the dipolar component and are relatively unimportant at geocentric distances of order one earth radius and beyond. Measurements made at the earth's surface, however, suggest that the dipole axis is tilted 11.4° relative to the rotation axis and displaced ~400 km from

the center of the earth[5]. True magnetic anomalies (deviations from a dipolar field) can originate either from higher multipoles of the core field or from concentrations of ferromagnetic material in the earth's crust. In addition, currents can be induced in the earth and in the ionosphere by virtue of the earth's rotation and by externally produced disturbances (see below) of the geomagnetic field. These induced currents can be very complicated in structure; fortunately, they are not known to have a dominant influence on the radiation belts.

The principal distortions of the earth's *outer* magnetosphere are caused by currents on the magnetopause, on the neutral sheet, and within the magnetosphere itself. The current layer that constitutes the magnetopause serves to confine the geomagnetic field within. Thus, the magnetopause is a boundary beyond which the earth's field does not extend. The neutral sheet, which separates the oppositely oriented flux tubes that constitute the geomagnetic tail, carries currents that tend generally to weaken the nightside field intensity. Together, the magnetopause and neutral sheet form the magnetospheric surface.

The final source of field distortion important for the radiation belts is the *ring current* carried by the hot component of the magnetospheric plasma. The direction of gradient-curvature drift in the earth's field is westward for protons and eastward for electrons, and indeed the *net* ring current flows *westward*. The result is a generally outward displacement of field lines, *i. e.*, a decreased magnetic-field intensity at the earth's surface and elsewhere interior to the ring-current zone, but an enhanced field strength at exterior points. With particle gyration taken into account, the spatial distribution of electric-current *density* is found to have a more subtle structure than consideration of gradient-curvature drift alone would suggest. For reasons discussed below, the local current density actually is directed eastward at the inner edge of the ring-current belt, but the net current carried by a spatially bounded hot plasma does flow westward, in accordance with the unsophisticated expectation.

It is generally considered impractical to model all the aforementioned current systems simultaneously and self-consistently. In studying radiation-belt dynamics by theoretical means, however, it is usually sufficient to recognize that self-consistent magnetic-field models exist in principle. Thus, it is possible to *imagine* the computation of a particle's three

[5]The 400-km displacement causes the apogee of an inner-zone particle drift shell to be located over the western Pacific Ocean. Conversely, perigee is attained over the south Atlantic. Since the field intensity at a given geocentric *altitude* over the south Atlantic is substantially smaller than at other geographic locations, this region where drift shells attain perigee is often called the *South Atlantic "anomaly"*.

adiabatic invariants and three phases with the understanding that these invariants and phases identify an equivalent "particle" trapped in the centered-dipole reference field. In particular, this mental exercise assigns to the particle a unique, significant, and adiabatically invariant shell parameter [5]

$$L = 2\pi a^2 B_0 |\Phi|^{-1}, \tag{1.37}$$

i.e., the shell parameter of the adiabatically equivalent "particle" in the dipole field.

The McIlwain Parameter. In most cases it is, in fact, necessary to carry out some form of adiabatic transformation of *observational* data so as to establish a requisite degree of order. In practice, quiet-time observations of the inner radiation zone ($L \lesssim 3$) need be corrected only for anomalies of the permanent geomagnetic field (including displacement of the point dipole). Since this field is constant over the lifetime of a typical satellite experiment, it is customary to circumvent computation of the invariant shell parameter given by (1.37). It is found that observational data from the inner zone can be ordered adequately by specifying the mirror field B_m and the second invariant J for particles of known energy. It is customary to derive from these quantities a non-invariant shell parameter L_m, defined as the dipole shell parameter of a "particle" having the same B_m, J, and energy. To facilitate the calculation of L_m, it is usual to introduce the quantity $I \equiv J/2p$. In a dipole field it is found that

$$y^2 (I^3 B_m / a^3 B_0) \equiv y^2 R = [Y(y)]^3 \tag{1.38}$$

where $y^2 = B_0 / L^3 B_m$. The shell parameter L_m is thus defined by the relation $L_m^3 = B_0 / y^2 B_m$, where y is the solution of (1.38). The value of I is computed within the framework of an empirical model of the permanent geomagnetic field[6], and the value of $R (\equiv I^3 B_m / a^3 B_0)$ is thereby determined [21].

Since the function $Y(y)$ given by (1.29) cannot be expressed in closed form by elementary functions, an exact algebraic solution of (1.38) for y is impossible to obtain. Moreover, the analytical approximation to $Y(y)$ given by (1.31) does not render (1.38) algebraically tractable as an equation to be solved for y. A numerical solution is possible, of

[6]The parameter L_m originally defined by McIlwain [21] is computed by assigning $B_0 = 0.311653$ gauss. However, it would be more reasonable to compute L_m using the best available field model and the corresponding value of B_0 for the epoch in question [22].

course, but for most purposes the empirically deduced relationship [22]

$$\begin{aligned} B_m L_m^3 / B_0 &\approx 1 + (18/\pi^2)^{1/2} R^{1/3} + 0.465380\, R^{2/3} + [Y(0)]^{-3} R \\ &\approx 1 + 1.350474\, R^{1/3} + 0.465380\, R^{2/3} + 0.047546\, R \end{aligned} \tag{1.39}$$

is entirely adequate for defining L_m in terms of I and B_m. Indeed, the error in using (1.39) to specify L_m amounts to less than 0.01%, as compared with the value of L_m obtained via the exact dipole function given by (1.29b). The coordinates B_m and L_m, generally called (B, L) coordinates, are known to order inner-zone particle data satisfactorily during magnetically quiet periods, in spite of certain conceptual difficulties; *e.g.*, the fact that (even in an azimuthally symmetric field) particles having the same Φ can be assigned different values of L_m. The utility of (B, L) space for describing the inner zone during quiet periods resides in the fact that such conceptual discrepancies are of insignificant magnitude there. For example, the variation of L_m (as computed from a standard 512-term multipole expansion of the permanent geomagnetic field) among particles whose mirror points lie along a given field line amounts consistently to less than 1% [21].

The Ring Current. During magnetically disturbed periods it is necessary to take adiabatic account of ring-current effects in both the inner ($L \lesssim 3$) and outer ($L \gtrsim 3$) radiation zones. As a very crude approximation, the ring current may be compared to a solenoid located beyond $L \approx 3$. This approximation suggests a roughly uniform field perturbation oriented parallel to the dipole axis and extending throughout the inner zone[7]. This perturbing field often attains a magnitude $\gtrsim 200\gamma$ during magnetic storms and is closely associated with the equatorial geomagnetic index D_{st}, which is supposed to measure the azimuthally symmetric component of the axial field perturbation induced by the storm [23]. The signature of D_{st} (as obtained from low-latitude magnetograms) is usually negative because the perturbing field points southward, thereby diminishing the field intensity at the earth's surface, where the equatorial dipolar component points generally northward. (On exceptional occasions, when the ring current is weak, a positive D_{st} can result from compression of the magnetosphere by the solar wind.)

During a magnetic storm the ring current tends to coexist spatially with a portion of the outer zone, and so it would be a poor approximation to extend the uniform perturbing field beyond $L \approx 3$. Indeed, within

[7]Temporal changes in the uniform axial field induce (via surface currents) an effective magnetic dipole in the earth, which is essentially a perfect conductor on the time scale of a geomagnetic storm.

the belt of ring-current protons and electrons, diamagnetic effects can accentuate the field depression beyond that seen at the earth's surface ($r=a$). On the outer fringes of the ring-current belt, the field depression is greatly reduced. At sufficiently large distances the ring current would resemble a magnetic dipole (of finite extent) aligned with the earth's dipole. The result is therefore an augmentation of the earth's field at such distances. Since self-constistent models of the ring current and its magnetic field [24] require considerable computation, it is customary to employ semi-empirical models to account for the associated adiabatic effects upon radiation-belt particles.

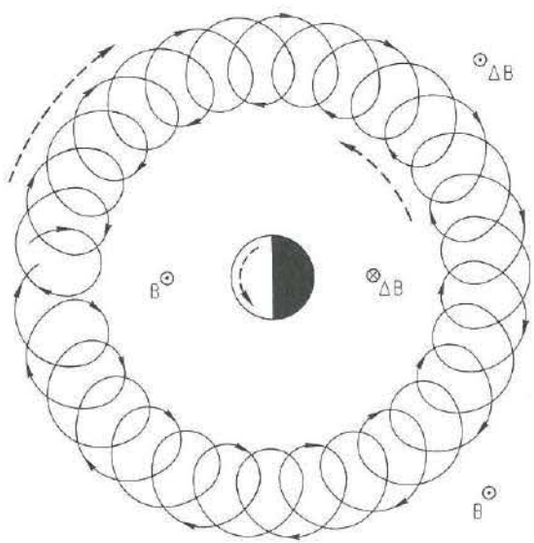

Fig. 8. Schematic representation of the gyration and azimuthal drift (solid curve) of an equatorially mirroring proton, with associated current patterns (dashed curves).

Figure 8 illustrates the drift-phase averaged current pattern associated with the gyration and gradient drift of an equatorially mirroring proton. The current pattern in this case has a width of two gyroradii. The inner portion of this pattern carries an eastward current, while the outer portion carries a somewhat larger westward current. The net flux of electrical current across each meridional half-plane is westward, as provided by the gradient drift. Formulation of a ring-current model consists of superimposing the contributions of all protons and electrons in the hot plasma, whose behavior is governed by the self-consistent field.

In a plasma having pressure $P_\perp$ in the direction normal to $\mathbf{B}$, the *magnetization current* (caused by particle gyration) has a density $\mathbf{J}_m = -c\nabla\times(P_\perp\mathbf{B}/B^2)$. Under nonrelativistic conditions, gradient drift produces a current density $\mathbf{J}_g = c(P_\perp/B^2)\hat{\mathbf{B}}\times\nabla B$, and curvature drift yields a current density $\mathbf{J}_c = c(P_{||}/B^2)\mathbf{B}\times(\partial\hat{\mathbf{B}}/\partial s)$, where $P_{||}$ is the component of plasma pressure parallel to $\mathbf{B}$. The magnetization current can be written in the expanded form

$$\mathbf{J}_m = -c(P_\perp/B^2)\nabla\times\mathbf{B} + (c/B^2)\mathbf{B}\times\nabla P_\perp - 2\mathbf{J}_g \tag{1.40a}$$

and the gradient-drift current can be expressed as

$$\mathbf{J}_g = c(P_\perp/B^2)[\mathbf{B}\times(\partial\hat{\mathbf{B}}/\partial s) - (\nabla\times\mathbf{B})_\perp]. \tag{1.40b}$$

In differential geometry the normal vector $\partial\hat{\mathbf{B}}/\partial s$ has a magnitude equal to the local curvature of the field line and points toward the center of curvature. Under the static conditions considered here, the total current density $\mathbf{J}$ satisfies the relation $c\nabla\times\mathbf{B} = 4\pi\mathbf{J} = 4\pi(\mathbf{J}_m+\mathbf{J}_g+\mathbf{J}_c)$ and is given [25] by

$$\mathbf{J} = (c/B)\hat{\mathbf{B}}\times\nabla P_\perp + (c/8\pi)(\beta_{||}-\beta_\perp)\mathbf{B}\times(\partial\hat{\mathbf{B}}/\partial s), \tag{1.41}$$

where $\beta_{||} = 8\pi P_{||}/B^2$ and $\beta_\perp = 8\pi P_\perp/B^2$. The beta parameters relate the pressures exerted by the hot plasma to that exerted by the magnetic field. Observations of the earth's ring current indicate that $\beta_{||}$ and $\beta_\perp$ both attain magnitudes of order unity in the region of space most densely populated by protons in the energy range 10—50 keV [15]. This region lies in the vicinity of $L=3$ during large magnetic storms and near $L=7$ during geomagnetically quiet times[8].

The initial term of (1.41) points in the eastward $(+\hat{\boldsymbol{\varphi}})$ direction in the inner portion of the ring-current zone, but in the westward $(-\hat{\boldsymbol{\varphi}})$ direction in the outer portion. Since $\hat{\mathbf{B}}\times\nabla P_\perp$ is weighted by $1/B$ in (1.41), the westward contribution predominates if the hot plasma is spatially bounded[9].

Simplified models of the ring-current field [26] can be constructed empirically, by allowing the field perturbation to have a fixed spatial profile whose amplitude is directly proportional to D_{st}. Such a model is illustrated in Fig. 9, where $\Delta\mathbf{B}$ is the *equatorial* $\mathbf{B}$-field perturbation caused by the ring current. As noted above, this total field perturbation

[8] High-beta conditions also characterize the vicinity of the dayside neutral points and the nightside neutral sheet. Elsewhere in the magnetosphere it is found that both $\beta_{||}$ and $\beta_\perp$ are rather small in comparison with unity.

[9] Similarly, the inner edge of the plasma sheet can carry an eastward current, even though the predominant flow of current on the neutral sheet is westward, in accordance with the expectation based on gradient drift.

includes the earth-induction field $\mathbf{B}_i$ which can be simulated by placing a point dipole at the geocenter. The ratio of B_i to the field of the earth's permanent dipole is very small, *i.e.*, approximately the ratio of D_{st} to one gauss. The form of $\Delta\mathbf{B}$ beyond $L\sim 3$ is not really independent of D_{st}, as the model implies. In fact, the diamagnetic field depression resides at $L\lesssim 4$ only when $|D_{st}|\gtrsim 100\gamma$. The region of maximum hot-plasma energy density is observed to be correlated with D_{st} in such a manner that beta attains a value of order unity there [15]. Thus, the diamagnetic depression moves outward in L with decreasing $|D_{st}|$. However, the ring current exerts a negligible influence on the radiation belts when D_{st} is smaller than $\sim 30\gamma$ in absolute value. The model summarized by Fig. 9 is therefore adequate in the sense that an accurate profile of $\Delta B/D_{st}$ is needed only for the rather large values of $|D_{st}|$ to which Fig. 9 applies.

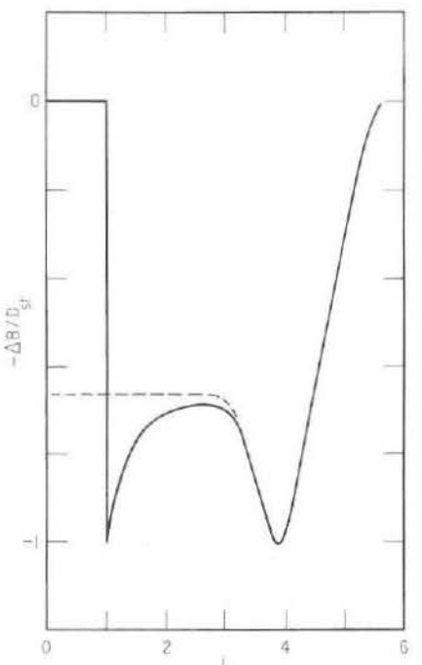

Fig. 9. Semi-empirical relationship between equatorial ring-current field ΔB and magnetic index D_{st} [26], including effects of currents induced on the surface of a perfectly conducting earth (solid curve); with such earth-induction field subtracted out (dashed curve).

The Mead Field. In addition to ring-current effects, the earth's magnetic field is permanently distorted by virtue of currents that flow on the magnetopause and neutral sheet. Various models are available for describing the effects of these currents in a quantitative manner [27, 28]. The permanent compression of the magnetosphere caused directly by the solar wind can best be evaluated by expanding a scalar potential function $V_m(r,\theta,\varphi)$ in spherical harmonics and deriving from this potential the magnetic field $\mathbf{B}=-\nabla V_m$. The coefficients introduced in the spherical-harmonic expansion are then evaluated by requiring pressure balance at the resulting magnetopause. This procedure is greatly simplified by supposing that the earth's dipole is normal to the direction of the undeflected solar wind. The use of a scalar potential $V_m(r,\theta,\varphi)$ implies the neglect of plasma-pressure effects (*e.g.*, currents) within the magnetosphere. Pressure balance at the magnetopause therefore requires that $B^2=8\pi\rho_s u^2(1-\cos\psi_s)$ at each point on this boundary, where ρ_s is the mass density of solar-wind material, $\mathbf{u}$ is the velocity of the undeflected solar wind, and ψ_s is the angle of deflection caused by encounter with the magnetopause. This formulation ignores the interplanetary magnetic field, whose energy density is smaller than that of the flowing plasma by a factor ~ 100.

A simplified picture of solar-wind deflection by the magnetopause postulates specular reflection of the plasma. In this case the angle ψ_s is twice the local angle of attack of the incident solar wind. The resulting coefficients $\bar{g}_l^m$ in the expansion

$$V_m(r,\theta,\varphi)=-B_0(a^3/r^2)\cos\theta+(a^3/b^2)\sum_{l=1}^{\infty}(r/b)^l\bar{g}_l^m P_l^m(\cos\theta)\cos m\varphi\,, \quad (1.42)$$

which exhibits north-south and dawn-dusk symmetry by virtue of the assumed orthogonality of $\mathbf{u}$ to the dipole axis, define the Mead field [28]. The symbol $P_l^m(\cos\theta)$ denotes an associated Legendre polynomial with Schmidt normalization[10], as is conventional for geomagnetic applications. The computed values of $\bar{g}_l^m/B_0$ are given in Table 2, and b is the equatorial "stand-off" distance from the point dipole to the magnetopause in the noon meridian. From the indicated coefficients it follows that

$$b=1.068\;\;B_0^2/4\pi\rho_s u^2)^{1/6}a, \quad (1.43)$$

so that $b\approx 10a$ under typical solar-wind conditions.

[10] The functions $P_l^m(x)$ are defined by the equations

$$P_l^m(x)=\left[\frac{2(l-m)!}{(l+m)!}\right]^{1/2}\frac{(1-x^2)^{m/2}}{2^l l!}\frac{d^{l+m}}{dx^{l+m}}[(x^2-1)^l], \quad m>0$$

$$P_l^m(x)=\frac{1}{2^l l!}\frac{d^l}{dx^l}[(x^2-1)^l], \quad m=0\,.$$

Table 2. Expansion Coefficients for Mead Field

l,m	$\bar{g}_l^m/B_0$	l,m	$\bar{g}_l^m/B_0$
1,0	0.8100	5,0	0.0184
2,1	0.4065	5,2	−0.0348
3,0	−0.0233	5,4	−0.0032
3,2	−0.0752	6,1	−0.0042
4,1	0.0775	6,3	0.0061
4,3	0.0052	6,5	0.0013

For illustrative purposes the potential given by (1.42) can be simplified further by neglecting those coefficients $\bar{g}_l^m$ that have $l>2$. The simplified potential can then be written [28] in the form

$$V_m(r,\theta,\varphi)=-B_0(a^3/r^2)\cos\theta-[B_1 z-B_2 z(x/b)](a/b)^3, \quad (1.44)$$

where $x=r\sin\theta\cos\varphi$, $z=r\cos\theta$, $B_0\approx 0.31$ gauss, $B_1=-\bar{g}_1^1\approx 0.25$ gauss, and $B_2=\sqrt{3}\bar{g}_2^1\approx 0.21$ gauss. Very often the simplified field derived from (1.44) can be utilized fruitfully in analytical calculations related to adiabatic motion and particle diffusion. In polar coordinates this simplified field has the form

$$B_r=-2B_0(a/r)^3\cos\theta+B_1(a/b)^3\cos\theta -2B_2(a/b)^4(r/a)\cos\theta\sin\theta\cos\varphi \quad (1.45\,a)$$

$$B_\theta=-B_0(a/r)^3\sin\theta-B_1(a/b)^3\sin\theta +B_2(a/b)^4(r/a)(2\sin^2\theta-1)\cos\varphi \quad (1.45\,b)$$

$$B_\varphi=B_2(a/b)^4(r/a)\cos\theta\sin\varphi\,, \quad (1.45\,c)$$

where r is the geocentric distance, θ is the colatitude measured from the northern pole, and φ is the east longitude measured from the midnight meridian. Figure 10 illustrates field-line traces for this model and the dipole field in the plane for which $\sin\varphi=0$. For this purpose field lines are identified by the label L_d, defined as the limit of $(r/a\sin^2\theta)$ as θ approaches zero. This definition is motivated by (1.17b).

The simplified Mead field given by (1.45) can be considered a special case of the general analytic representation [29]

$$B_r(r,\theta,\varphi;t)=\sum_{lmn}B_r(l,m,n;t)(r/a)^n\cos\theta\sin^l\theta\cos m\varphi \quad (1.46\,a)$$

$$B_\theta(r,\theta,\varphi;t)=\sum_{lmn}B_\theta(l,m,n;t)(r/a)^n\sin^l\theta\cos m\varphi \quad (1.46\,b)$$

$$B_\varphi(r,\theta,\varphi;t)=\sum_{lmn}B_\varphi(l,m,n;t)(r/a)^n\cos\theta\sin^l\theta\sin m\varphi \quad (1.46\,c)$$

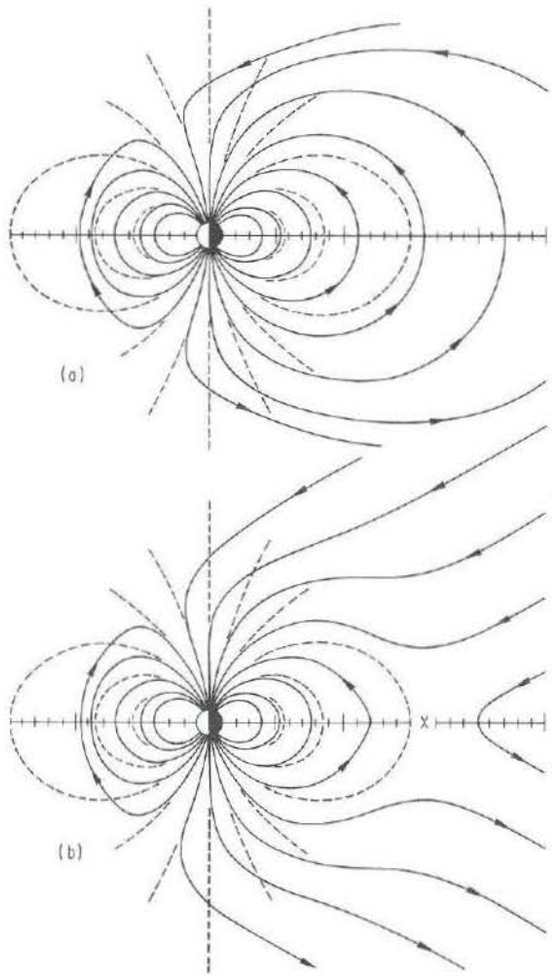

Fig. 10. Schematic representation of meridional field lines in (a) the 13-term and (b) the 3-term magnetospheres (solid curves). Corresponding dipole field lines (dashed curves) are shown for $\Lambda=65°$, 70°, 75°, 80°, 85°, and 90°, but omitted for $\Lambda=60°$, where $\Lambda\equiv\sec^{-1}(L_d^{1/2})$. The symbol X marks the location of the nightside neutral line that automatically appears in the 3-term model.

of a magnetic field having symmetry with respect to the equatorial plane and the noon-midnight meridional plane. The completeness of (1.46) as the expansion of an analytic function having these symmetries is quite evident. The radial variable r enters in the form of a Taylor-Laurent series. Functions of the colatitude θ that are even with respect

to $\theta=\pi/2$ can surely be written as a power series in $\sin\theta$. As for functions that are odd with respect to $\theta=\pi/2$, the factor $\cos\theta$ need enter only to the first power, since even powers of $\cos\theta$ can be written as polynomials in $\sin\theta$. Finally, a Fourier series in $\sin m\varphi$ or $\cos m\varphi$ will suffice to express an analytic function that is odd or even with respect to the midnight meridian ($\varphi=0$).

Since (1.46) is considerably more general than a spherical-harmonic expansion of $V_m(r,\theta,\varphi;t)$, it can be used even in the presence of ring currents and other distributed sources. All that is required for this extension is that care be taken to satisfy the relation $c\nabla\times\mathbf{B}=4\pi\mathbf{J}+(\partial\mathbf{E}/\partial t)$, where $\mathbf{E}$ is the electric field and $\mathbf{J}$ is the current density. In addition to this requirement, of course, the magnetic field must be made to satisfy $\nabla\cdot\mathbf{B}=0$ under all conditions. This general requirement leads to the constraining equation

$$(n+2)\,B_r(l-1,m,n;t)+(l+1)\,B_\theta(l,m,n;t)+m\,B_\varphi(l,m,n;t)=0\,, \quad (1.47)$$

which indeed is satisfied by the coefficients

$$B_r(0,0,-3)=2\,B_\theta(1,0,-3)=-2\,B_0 \quad (1.48\,a)$$

$$B_r(0,0,0)=-B_\theta(1,0,0)=B_1\,(a/b)^3 \quad (1.48\,b)$$

$$B_r(1,1,1)=2\,B_\theta(0,1,1)=-B_\theta(2,1,1)=-2\,B_\varphi(0,1,1)=-2\,B_2\,(a/b)^4 \quad (1.48\,c)$$

$$B_0=1.24\,B_1=1.48\,B_2=0.31 \text{ gauss} \quad (1.48\,d)$$

appropriate to the simplified Mead model given by (1.45). As noted above, the simplified field is especially useful for carrying out analytical calculations appropriate to a model magnetosphere. In some cases however, the simplified model is not accurate enough to organize observational data obtained beyond $L\approx 5$, *i.e.*, to recast such data in terms of a standard magnetosphere by means of the required adiabatic transformations.

The Mead-Williams Field. The usual shortcoming of (1.45) in the description of observational data is the neglect of the neutral-sheet currents associated with the geomagnetic tail. In principle, these currents fit into the framework of (1.46) so long as they are distributed in space rather than confined to an idealized sheet of vanishing thickness. In other words, so long as $\mathbf{J}$ is everywhere finite in magnitude, there are no singularities in $\mathbf{B}$ that (1.46) fails to handle. In practice, however, it is customary to represent the neutral sheet in the idealized manner. This means that the Mead field (typically as derived from Table 2) is augmented by the field of a current-carrying sheet located on the

nightside equator. Various representations are possible. The popular Mead-Williams field [30] represents the current sheet as a strip of finite width ($x=x_n$ to $x=x_f$, subscripts denoting the near and far boundaries) extending from $y=-\infty$ to $y=+\infty$ (see Fig. 3). The current is assumed to be distributed uniformly between $x=x_n$ and $x=x_f$ and flows from $y=+\infty$ (east) to $y=-\infty$ (west). Near the current sheet itself, the resulting tail field $\mathbf{B}_t$ has a magnitude

$$B_t=(2\pi/c)(x_f-x_n)^{-1}\,I\,, \quad (1.49)$$

where I is the total current carried. This field points sunward ($-\hat{\mathbf{x}}$) in the northern hemisphere and antisunward ($+\hat{\mathbf{x}}$) in the southern hemisphere. As a result, nightside polar field lines (*i.e.*, those emanating from the earth at polar latitudes) are greatly extended in the equatorial region.

With the aid of a system of synchronous satellites ($r=6.6a$, $\dot{\varphi}=2\pi/\text{day}$) it becomes possible to compile a magnetospheric "weather report" providing both b (the stand-off distance) and B_t (the tail field) as functions of time. The method is to compare the observed magnetometer readings at various longitudes with those predicted by assuming various combinations of the two model parameters. The determination of b and B_t is made most confidently by comparing equatorial values of B at $\varphi=0$ (midnight) and $\varphi=\pi$ (noon). The model parameters are then defined by locating B_e ($\varphi=0$) and B_e ($\varphi=\pi$) in Fig. 11, which is a contour plot of b and B_t [31]. In case multiple-satellite coverage is not available at the synchronous orbit, it may be necessary to utilize

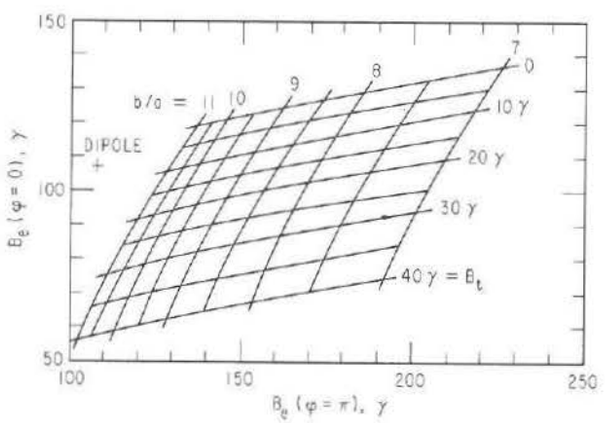

Fig. 11. Equatorial magnitudes of $\mathbf{B}$ at noon ($\varphi=\pi$) and midnight ($\varphi=0$) in synchronous orbit ($r=6.6a$) computed [31] for selected values of the Mead-Williams parameters b/a and B_t [30], with $x_n/a=10.6-0.06(B_t/1\gamma)$ and $x_f/a=200$.

readings of a single magnetometer taken at twelve-hour intervals for the purpose outlined above. This procedure is acceptable as long as magnetospheric conditions do not change significantly during the twelve-hour interval between midnight and noon [31]. Using the report of the day-to-day variation of b and B_t obtained by this method, it is possible to recast particle data obtained beyond $L \approx 3$ in terms of a standard magnetosphere, *e. g.*, the dipole field. In this case each particle in the distorted field is to be identified with an equivalent "particle" having the same three adiabatic invariants and phases (but probably a different pitch angle and energy) in the dipole field. For $L \lesssim 5$ it is usually unnecessary to make such a transformation, as the effects of currents on the magnetopause and neutral sheet are small in magnitude there, when compared with the magnitude of the dipole field (see Section 1.4).

There exists some doubt that the subsolar point $(r, \theta, \varphi) = (b, \pi/2, \pi)$ on the magnetopause should be treated as a point of specular reflection (as in the Mead model) rather than a point of hydrodynamic stagnation [10]. The truth presumably lies somewhere between these two limits. If ρ_s is the density of mass flowing at the solar-wind velocity $\mathbf{u}$, pressure balance at the subsolar point is expressed by the relation $\rho_s u^2 = B^2/4\pi$ for specular reflection and by $\rho_s u^2 = B^2/8\pi$ for hydrodynamic stagnation. The superficial consequence of the uncertainty involved here is a possible error $\sim 12\%$ in specifying b by means of (1.43); a deeper consideration of the hydrodynamic model would require a difficult recomputation of the coefficients $\bar{g}_l^m$ that appear in Table 2. Existing problems in the field of radiation-belt dynamics, however, appear to transcend such subtleties in modeling the magnetosphere.

Similarly, a more realistic model of the tail field might take into account the fact that the relevant current loops close over the cylindrical surface of the magnetosphere rather than at infinity. By thus restricting the current sheet to a lateral dimension $\lesssim 4b$, it is possible to extend x_f to infinity, or at least to realistically large distances ($\gtrsim 50b$) without catastrophe to the dayside magnetosphere. An additional element of reality would be introduced by taking account of the tilt that exists between the earth's dipole and the solar wind. Since the dipole axis is inclined 11.4° to the rotation axis, which in turn is inclined 22.5° to the ecliptic plane, the tilt of the dipole away from normal solar-wind incidence can amount to as much as 34°, depending on time of day and season of year. In recent years considerable progress has been made toward constructing models that account for the influence of tilt on the shape of the magnetopause, the character of the distorted field, and the position of the neutral sheet. As with the questions raised in the paragraph above, it appears that these considerations are quite

important in defining the overall structure of the magnetosphere (including, for example, the description of diurnal and seasonal variations characteristic of ground-based magnetometer readings), but that these complicating effects are not of crucial importance to the radiation belts *per se*. In other words, the existing state of knowledge concerning the earth's trapped-radiation environment does not justify the additional labor inherent in more realistically describing the containing magnetic field for radiation-belt studies. Accordingly, the field models employed in subsequent analyses will be kept as simple as possible.

I.6 Magnetospheric Electric Fields

Large-scale electric fields in the magnetosphere originate primarily from temporal variations of the magnetic field, from the rotation of the earth, and from plasma instabilities of the neutral sheet. Electric fields induced by temporal variations of $\mathbf{B}$ are not derivable from an electrostatic (scalar) potential V_e, because $c\nabla \times \mathbf{E} = -\partial \mathbf{B}/\partial t$. Those resulting from the earth's rotation and from neutral-sheet instabilities can be derived from scalar potentials. The electrostatic field caused by the rotation of a magnetic dipole about its axis, taken as an idealized geophysical situation, is given by

$$\begin{aligned} \mathbf{E} &= -(1/c)(\boldsymbol{\Omega}_0 \times \mathbf{r}) \times \mathbf{B} \\ &= B_0(\Omega_0 a/c)(2\hat{\boldsymbol{\theta}}\cos\theta - \hat{\mathbf{r}}\sin\theta)(a/r)^2 \sin\theta \end{aligned} \tag{1.50}$$

where $\boldsymbol{\Omega}_0$ is the angular velocity of the earth. This field can be derived from the potential

$$V_e(r, \theta, \varphi) = -B_0 \Omega_0 a^2 / c L_d, \tag{1.51a}$$

where

$$L_d \equiv \lim_{\theta \to 0} (r/a \sin^2\theta). \tag{1.51b}$$

The limit indicated in (1.51 b) must be evaluated along the magnetic field line. The field-line label L_d proves to be useful in other applications in which internal geomagnetic multipoles are neglected, *e. g.*, those involving the Mead field, hence the need for a precise definition. A dipole field line, of course, identically satisfies the relation $r = L_d a \sin^2\theta$.

The so-called convection electric field $\mathbf{E}_c$ required to maintain the tail (neutral-sheet) current in the presence of intrinsic plasma turbulence is customarily represented via the potential

$$V_c(r, \theta, \varphi) = E_c a L_d \sin\varphi \tag{1.52}$$

in the region where **B** is dipolar. This expression reduces to $V_e(r,\pi/2,\varphi) = E_c y$ in the equatorial plane, where the idealized field attains the spatially uniform (in two dimensions) magnitude E_c, directed from dawn to dusk ($-\hat{\mathbf{y}}$). This field drives a sunward ($-\hat{\mathbf{x}}$) convection of plasma in the forward portion of the magnetosphere, where $\hat{\mathbf{B}}=\hat{\mathbf{z}}$ in the equatorial plane. The plasma flow follows from the standard relation

$$\mathbf{v}_d=(c/B^2)\mathbf{E}\times\mathbf{B}. \tag{1.53}$$

In the magnetotail, however, the general direction of **B** is either $-\hat{\mathbf{x}}$ (northern hemisphere; $z>0$) or $+\hat{\mathbf{x}}$ (southern hemisphere; $z<0$). The result is a plasma flow velocity

$$\mathbf{v}_d=-\hat{\mathbf{z}}(cE_c/B_t)(z/|z|) \tag{1.54}$$

directed into the neutral sheet.

A picturesque interpretation of (1.54) is that the field lines themselves flow into the neutral sheet at a speed cE_c/B_t, there experiencing a mutual annihilation that liberates energy at a rate of $2(B_t^2/8\pi)(cE_c/B_t)$ per unit area since $B_t^2/8\pi$ is the density of field energy. Similarly, it is possible to view sunward convection of plasma as a "snapping back" of field lines that have been dragged downstream by a viscous interaction with the solar wind. Indeed, there exists such a viscous interaction at the magnetopause, but it acts fundamentally upon the *plasma* rather than upon the *field* [12]. Plasma and field-line motion can be identified in terms of (1.53) by requiring also that $\mathbf{E}=-(1/c)\mathbf{v}_d\times\mathbf{B}$ [see (1.50)]. There exists, then, a choice between postulating field-line motion at velocity $\mathbf{v}_d$ accompanied by plasma motion at the same velocity (line tying) on the one hand, and the convection of plasma at velocity $\mathbf{v}_d$ across a stationary **B** field on the other.

Particularly in the steady state, for which $\partial\mathbf{B}/\partial t=0$, the dual concepts of field-line motion and line tying can be very confusing when taken as a foundation for quantitative analysis. The description based on physically measurable quantities such as **E** and **B** is never less adequate than the more colorful description, and usually yields more readily to quantification.

The electrostatic fields derived from (1.51) and (1.52) have the property that $\mathbf{E}\cdot\mathbf{B}=0$, where **B** is given by (1.16). The property $\mathbf{E}\cdot\mathbf{B}=0$ seems to be essential for the identification of field-line motion with cold-plasma motion [32]. Accordingly, it has become conventional to postulate the condition $\mathbf{E}\cdot\mathbf{B}=0$ as a means of mapping magnetospheric electric fields. The usual rationale for this postulate is that the magnetosphere contains cold plasma of sufficient density to short out any appreciable

field-aligned component of **E** [11][11]. Applicability of the condition $\mathbf{E}\cdot\mathbf{B}=0$ anywhere beyond the plasmasphere is a matter of some controversy, although (as noted) this procedure is the conventional one for mapping magnetospheric electric fields [33].

It is inappropriate to employ (1.51) and (1.52) where the magnetic field differs significantly from that of a dipole. One prescription for obtaining **E** in the distorted field involves an expansion analogous to (1.46). This prescription defines an iterative procedure [34] whereby the condition $\mathbf{E}\cdot\mathbf{B}=0$ is imposed order by order in r/b, beginning with (1.50).

Operating within the framework of the dipole field, it is not difficult to establish the existence of both closed and open equipotential surfaces of the superimposed convection and corotation electric fields. The total electrostatic potential of this idealized steady-state magnetosphere has the form

$$V_e(r,\theta,\varphi)=E_c L_d a\sin\varphi-B_0(\Omega_0 a^2/cL_d), \tag{1.55}$$

and so equipotential (constant-V_e) surfaces are specified by

$$L_d=(2E_c a\sin\varphi)^{-1}\{V_e\pm[V_e^2+(4E_c B_0\Omega_0 a^3/c)\sin\varphi]^{1/2}\}. \tag{1.56}$$

Examples are illustrated in Fig. 12; the singular equipotential surface that separates the closed and open cold-plasma drift shells is that for which $V_e=-2(E_c B_0\Omega_0 a^3/c)^{1/2}$. This shell, which satisfies the equation

$$L_d=(B_0\Omega_0 a/cE_c)^{1/2}[(1+\sin\varphi)^{1/2}-1]\csc\varphi, \tag{1.57}$$

is closely associated with a virtual discontinuity in the magnetospheric cold-plasma density. The underlying reason for this *plasmapause* is that ionospheric plasma originating at low and middle latitudes remains trapped within closed equipotential surfaces, while that originating at sufficiently high latitudes proceeds to escape from the magnetosphere.

The dimensionless parameter $(B_0\Omega_0 a/cE_c)^{1/2}$ appearing in (1.57) measures (in earth radii) the nominal radius of the plasmasphere. More precisely, this parameter identifies the equatorial geocentric distance to the plasmapause at the dusk meridian ($\varphi=-\pi/2$), which in this idealized model corresponds to the "bulge" region, *i.e.*, the region of maximum geocentric radius. A plasmasphere *diameter* of six earth radii in the noon-midnight meridian corresponds to a *radius* of six earth radii at dusk in this model, and leads to the estimate that $E_c\sim 4\,\mu$V/cm

[11] Beyond the radiation belts, *e.g.*, in the auroral zone, violations of this rule are quite common. The auroral zone appears to be associated with the earthward portion of the plasma sheet.

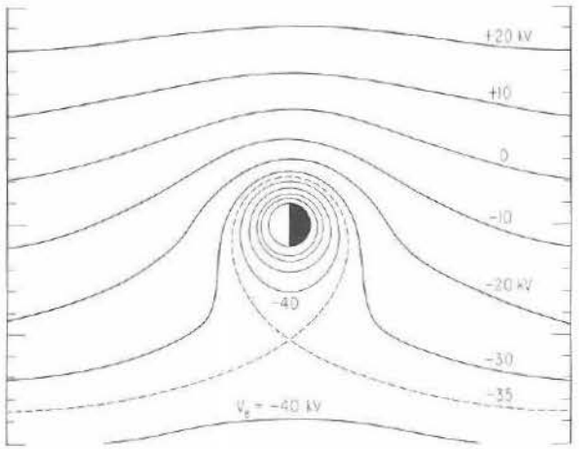

Fig. 12. Electrostatic equipotential contours in the equatorial plane of the idealized geomagnetic dipole, computed for $E_c = 0.526$ V/km (contours are unlabeled for $V_e < -40$ kV and omitted for $V_e < -70$ kV).

under typical conditions. In reality, the plasmasphere exhibits a somewhat less pronounced azimuthal asymmetry, and the "bulge" appears roughly midway through the evening quadrant ($\varphi \sim -\pi/4$). This means that (1.52) somewhat oversimplifies the actual convection electric field. Moreover, the size of the plasmasphere [see (1.57)] is found empirically to vary with magnetic activity (*e.g.*, with the geomagnetic index K_p) in a manner compatible with the statistical relationship [35]

$$E_c \approx 5.65\,(m_e c^2/q_p a)(u/c), \tag{1.58}$$

where m_e is the mass of an electron, q_p is the charge of a proton, and u is the solar-wind speed. This formula yields $E_c \approx 6\,\mu$V/cm for $u = 400$ km/sec. A statistical correlation between E_c and u is intuitively appealing in that sunward convection of plasma is supposed to balance (on average) the outward flow characteristic of a viscous boundary layer at the magnetopause [12].

The steady component of the magnetospheric electric field imposes a final restriction on radiation-belt particle energies. Convention requires that gradient-curvature drifts dominate adiabatic $\mathbf{E} \times \mathbf{B}$ drifts, at least to the point of guaranteeing existence of the third invariant; *i.e.*, a closed drift shell (see Introduction). Preferably, the particle energy should be large enough that the drift shell deviates insignificantly from that calculated in the absence of magnetospheric electric fields. This condition imposes the requirement that $E/L \gg |q|\,E_c a \sim 4$ keV (see above) and demarcates the outer radiation belt from the ring-current belt, with which

it is spatially coincident. Within the plasmasphere, however, it is necessary to operate in a frame rotating with the earth unless $EL \gg |q|\,B_0 \Omega_0 a^2/c \sim 100$ keV [see (1.51)]. Particles not satisfying this criterion should probably be excluded from consideration, since the usual radiation-belt methods and scaling laws (*e.g.*, Fig. 6) do not apply without this modification. Figure 13 summarizes the parametric demarcations that distinguish radiation-belt particles from the other inhabitants of the earth's magnetosphere, based on the various considerations outlined in the present chapter.

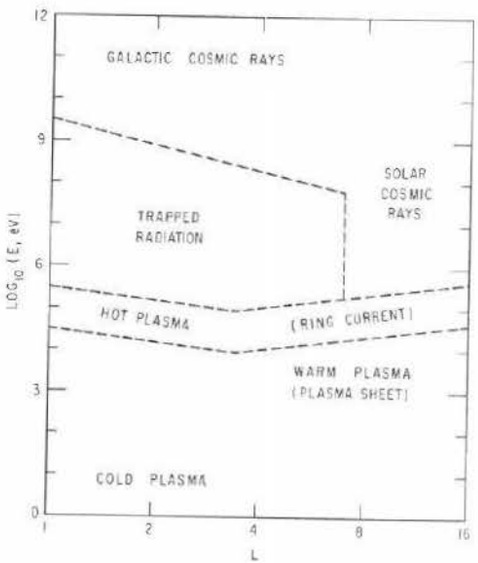

Fig. 13. Spatial and spectral classification of charged particles in the magnetosphere.

I.7 Flux Mapping and Shell Tracing

As a general rule, the particle flux $J_x(E;\mathbf{r})$ per unit energy E per unit solid angle Ω at local pitch angle α is related to the distribution function $f(p_\parallel, p_\perp;\mathbf{r})$ of (1.12) by the formula

$$J_x(E;\mathbf{r})\,dE\,d\Omega = f(p_\parallel, p_\perp;\mathbf{r})(p/m)p^2\,dp\,d\Omega, \tag{1.59}$$

where $m = \gamma m_0$ is the relativistic mass and m_0 is the rest mass. The total energy $mc^2 = E + m_0 c^2$ is related to the scalar momentum p by the equation

$$(E + m_0 c^2)^2 = p^2 c^2 + m_0^2 c^4 = p_\parallel^2 c^2 + p_\perp^2 c^2 + m_0^2 c^4, \tag{1.60}$$

where $p_{\|}=p\cos\alpha$ and $p_{\perp}=p\sin\alpha$. From (1.60) it follows that $m\,dE=p\,dp$, and so (1.59) becomes

$$J_{\alpha}(E;\mathbf{r})=p^2 f(p_{\|},p_{\perp};\mathbf{r}). \tag{1.61}$$

This equation is specialized to the case of locally mirroring particles by requiring $p_{\|}=0$ ($\alpha=\pi/2$), so that

$$J_{\perp}(E;\mathbf{r})=2m_0 MBf(0,p_{\perp};\mathbf{r}). \tag{1.62}$$

Since Liouville's theorem (Section I.3) assures that $f(p_{\|},p_{\perp};\mathbf{r})$ remains constant along a dynamical trajectory in phase space, conservation of the first adiabatic invariant means that $J_{\perp}/B$ at constant M remains fixed along the trajectory of a representative particle's mirror point in either hemisphere.

In an azimuthally symmetric magnetosphere, the tracing of drift shells would be very simple. Each shell could be generated by rotating a field line about the axis of symmetry. Particles mirroring at different latitudes along a given field line would proceed to generate coincident drift shells in the course of adiabatic motion, and the equatorial pitch angle of each particle would remain unchanged with azimuthal drift.

In the earth's magnetosphere, this azimuthal degeneracy is broken not only by the day-night asymmetry of the **B** field, as represented by (1.45), but also (to a lesser extent for radiation-belt particles) by the dawn-dusk asymmetry of the convection electric field, as represented by (1.52). As a consequence, the drift shells generated by the adiabatic motion of particles identical in species and energy, sharing a common field line at some longitude, generally do not coincide at other longitudes if the particles have different pitch angles at the equator of the common field line. This adiabatic phenomenon is known as *shell splitting* [5]. The extent to which drift shells are split by the azimuthal asymmetries can be judged by independently tracing the shells that correspond to distinct equatorial pitch angles $\sin^{-1}y$ on the common field line. It is instructive to consider the two dominant asymmetries separately.

Electric Shell Splitting. When the electrostatic potential given above by (1.55) is superimposed on the magnetic-dipole field (1.16), the tracing of drift shells is accomplished by employing conservation of $J=2L_d a\cdot p\,Y(y)$, $M=p^2/2m_0 B_m$, and $J^2/8m_0 a^2 M=B_m L_d^2 Y^2$, where $B_m=B_0/L_d^3 y^2$. The conserved energy $W\equiv E+qV_e(\mathbf{r})$ is given by

$$2m_0 c^2 MB_m+m_0^2 c^4=(m_0 c^2+W-qV_e)^2. \tag{1.63}$$

From these identities follow the differential relationships

$$(1/B_m)(dB_m/d\varphi)=-(2/L_d)(dL_d/d\varphi)-(2/Y)(dy/d\varphi)Y'(y), \tag{1.64a}$$

$$(2/y)(dy/d\varphi)=-(3/L_d)(dL_d/d\varphi)-(1/B_m)(dB_m/d\varphi), \tag{1.64b}$$

and

$$m_0 c^2 M(dB_m/d\varphi)= -q(m_0 c^2+W-qV_e)[(\partial V_e/\partial L_d)_{\varphi}(dL_d/d\varphi)+(\partial V_e/\partial\varphi)_{L_d}]. \tag{1.64c}$$

Taken together, equations (1.64) and (1.30) yield the drift-shell equations

$$dL_d/d\varphi=L_d T(y)(m_0 c^2+W-qV_e)[3(W-qV_e)(2m_0 c^2+W-qV_e)D(y) -T(y)(m_0 c^2+W-qV_e)q(\partial V_e/\partial L_d)_{\varphi}]^{-1}q(\partial V_e/\partial\varphi)_{L_d} \tag{1.65a}$$

$$dy/d\varphi=-(y/4L_d)[Y(y)/T(y)](dL_d/d\varphi). \tag{1.65b}$$

Thus, evolution of the drift trajectory $L_d(\varphi)$ clearly depends upon y, and so the nonvanishing of $(\partial V_e/\partial\varphi)_{L_d}=E_e a L_d\cos\varphi$ leads to the splitting of drift shells. In the limit of very weak shell splitting ($|qV_e|\ll W$), the lowest-order approximation

$$L_d(\varphi)\approx L_d(0)\{1+[(m_0 c^2+W)/(2m_0 c^2+W)] \times(qE_e a L_d/3W)[T(y)/D(y)]\sin\varphi\} \tag{1.66}$$

follows from (1.65). The ratio T/D is a monotonically decreasing function of y.

Magnetic Shell Splitting. For sufficiently small absolute values of the expansion parameter $qE_e a L_d/W$, the shell splitting predicted by (1.66) is negligible compared with that caused by azimuthal asymmetry of the *magnetic* field. To evaluate this latter effect, it is proper to neglect $V_e(\mathbf{r})$ and calculate the energy-independent drift shells imposed by (1.45). In this case the expansion parameter $\varepsilon_2\equiv(B_2/B_0)(L_d a/b)^4\ll 1$ characterizes the azimuthal asymmetry. With the neglect of $V_e(\mathbf{r})$, the variables p and B_m become constants of the motion in a static **B** field. It is necessary, however, to generalize from the dipole functions $T(y)$ and $Y(y)$ so that $2\pi/\Omega_2$ and J can be written

$$2\pi/\Omega_2=4L_d a(m/p)\tilde{T}(y;L_d,\varphi) \tag{1.67a}$$

$$J=2L_d a p\,\tilde{Y}(y;L_d,\varphi). \tag{1.67b}$$

The derivation leading to (1.30) equally well relates $\tilde{Y}(y;L_d,\varphi)$ to $\tilde{T}(y;L_d,\varphi)$. Generalization of (1.28) to the non-dipolar **B** field (1.45) requires at least that $\tilde{T}(0;L_d,\varphi)$ and $\tilde{T}(1;L_d,\varphi)$ be calculated to lowest order in $\varepsilon_1\equiv(B_1/B_0)(L_d a/b)^3$ and $\varepsilon_2\equiv(B_2/B_0)(L_d a/b)^4$. The results are given by

$$\tilde{T}(0; L_d, \varphi) = 1 + (I_1/2) + \varepsilon_1 (15 I_9 - 16 I_7) - \varepsilon_2 (147 I_{12} - 205 I_{10} + 54 I_8) \cos\varphi \quad (1.68\text{a})$$

$$\tilde{T}(1; L_d, \varphi) = (\pi/6)\sqrt{2}\,[1 + \varepsilon_1 - (25\varepsilon_2/14)\cos\varphi]\,, \quad (1.68\text{b})$$

where

$$I_n \equiv \int_0^{\pi/2} \frac{\sin^n\theta\, d\theta}{(1+3\cos^2\theta)^{1/2}}\,, \quad (1.68\text{c})$$

and follow from a tracing of field lines that deviate from the dipole solution $r = L_d a \sin^2\theta$. To lowest order in ε_1 and ε_2, the distorted field lines satisfy the equations

$$d\ln r/d\theta = B_r/B_\theta = 2\,\mathrm{ctn}\,\theta - 3\varepsilon_1 \sin^5\theta\cos\theta + 2\varepsilon_2(3\sin^2\theta - 1)\sin^6\theta\cos\theta\cos\varphi \quad (1.69\text{a})$$

$$r = L_d a \sin^2\theta [1 - (\varepsilon_1/2)\sin^6\theta + (2\varepsilon_2/21)(7\sin^2\theta - 3)\sin^7\theta\cos\varphi]\,. \quad (1.69\text{b})$$

The functional value of $\tilde{T}(0; L_d, \varphi)$ is defined by the requirement that $L_d a\,\tilde{T}(0; L_d, \varphi)$ be equal to half the arc length of the entire field line, *i.e.*,

$$L_d a\,\tilde{T}(0; L_d, \varphi) = \int_0^{\pi/2} [r^2 + (dr/d\theta)^2 + r^2\sin^2\theta(d\varphi/d\theta)^2]^{1/2}\, d\theta\,. \quad (1.70)$$

Since $(d\varphi/d\theta)^2$ is of higher order than first in ε_2, this contribution to the arc length is neglected in obtaining (1.68a) directly from (1.69) and (1.70). Numerical values of I_n are listed in Table 3, together with the specific combinations needed in (1.68a).

The derivation of (1.68b) follows that of (1.28c). The harmonic bounce approximation requires that $(\partial^2 B/\partial s^2)$ defined as $\hat{\mathbf{B}}\cdot\nabla(\hat{\mathbf{B}}\cdot\nabla B)$, be evaluated on the magnetic-equatorial surface, *i.e.*, on the surface for which $\partial B/\partial s = 0$ and $\partial^2 B/\partial s^2 > 0$. For $\mathbf{B}$ given by (1.45) and $r \lesssim 0.8b$ this surface coincides with the plane $\theta = \pi/2$. A general expression for $\partial^2 B/\partial s^2$ at $\theta = \pi/2$, applicable whenever $\mathbf{B}$ is derivable from a scalar potential and has north-south symmetry about this plane, is

$$B r^2(\partial^2 B/\partial s^2) = 2r^2(\partial B/\partial r)^2 + 3B(\partial B/\partial r) + B^2 + 2(\partial B/\partial\varphi)^2 + B_\theta(\partial^2 B_\theta/\partial\theta^2)\,. \quad (1.71)$$

In particular, if $\mathbf{B}$ is given by (1.45), the result is

$$B r^2(\partial^2 B/\partial s^2) = 9B^2 - 9B_1(a/b)^3[3B - 2B_1(a/b)^3] + 2B_2^2(a/b)^6(r/b)^2(1+15\cos^2\varphi) + B_2(a/b)^3(r/b)[39B - 48B_1(a/b)^3]\cos\varphi \quad (1.72)$$

at $\theta = \pi/2$. Taken to lowest order ε_1 and ε_2, this result combines with (1.69b) to yield

$$B^{-1/2}(\partial^2 B/\partial s^2)^{1/2} = (3/L_d a)[1 - \varepsilon_1 + (25\varepsilon_2/14)\cos\varphi]\,. \quad (1.73)$$

Since $\Omega_2^2 = (p^2/2m^2 B)(\partial^2 B/\partial s^2)$ according to (1.26), it follows from (1.67a) and (1.73) that $\tilde{T}(1; L_d, \varphi)$ is correctly specified by (1.68b).

It is consistent with (1.30) to express the functions $\tilde{T}(y; L_d, \varphi)$ and $\tilde{Y}(y; L_d, \varphi)$ in the form

$$\tilde{T}(y; L_d, \varphi) = \tilde{T}(0; L_d, \varphi) + \varepsilon_1 y^2 G_1'(y) + \varepsilon_2 y^2 G_2'(y)\cos\varphi - (1/2)[\tilde{T}(0; L_d, \varphi) - \tilde{T}(1; L_d, \varphi)](y + y^{1/2}) \quad (1.74\text{a})$$

$$\tilde{Y}(y; L_d, \varphi) = (2 + y\ln y - 2y^{1/2})\,\tilde{T}(0; L_d, \varphi) - (2y + y\ln y - 2y^{1/2})\,\tilde{T}(1; L_d, \varphi) - 2\varepsilon_1 y G_1(y) - 2\varepsilon_2 y G_2(y)\cos\varphi\,, \quad (1.74\text{b})$$

where $G_1(1) = G_1'(1) = G_2(1) = G_2'(1) = 0$. Except for these four end-point constraints dictated by (1.68), the functions $G_1(y)$ and $G_2(y)$ remain to be specified (see below).

The drift-shell equation for constant p and B_m $(= B_e/y^2)$ is obtained by invoking the constancy of J [given by (1.67b)]; it follows that

$$dL_d/d\varphi = -[(\partial B_e/\partial\varphi)_{L_d}(\tilde{Y} - 2\tilde{T}) + 2B_e(\partial\tilde{Y}/\partial\varphi)_{L_d}] \div [2(B_e/L_d)\tilde{Y} + 2B_e(\partial\tilde{Y}/\partial L_d)_\varphi + (\partial B_e/\partial L_d)_\varphi(\tilde{Y} - 2\tilde{T})]\,, \quad (1.75)$$

where B_e is the field intensity at $\theta = \pi/2$. From (1.45b) and (1.69b) it follows that

$$B_e = (B_0/L_d^3)[1 + (5\varepsilon_1/2) - (15\varepsilon_2/7)\cos\varphi]\,. \quad (1.76)$$

Table 3. Selected Integrals I_n

$I_1 = 0.760346$	$I_7 = 0.406500$	$I_{13} = 0.315466$
$I_2 = 0.630306$	$I_8 = 0.385465$	$I_{14} = 0.305646$
$I_3 = 0.553737$	$I_9 = 0.367590$	$I_{15} = 0.296713$
$I_4 = 0.501251$	$I_{10} = 0.352080$	$I_{16} = 0.288537$
$I_5 = 0.462142$	$I_{11} = 0.338446$	$I_{17} = 0.281016$
$I_6 = 0.431423$	$I_{12} = 0.326330$	$I_{18} = 0.274066$

$$1 + (1/2)I_1 = 1.380173$$
$$15 I_9 - 16 I_7 = -0.988542$$
$$147 I_{12} - 205 I_{10} + 54 I_8 = -3.390834$$

If (1.75) is then evaluated to lowest order in the field asymmetry, the result is

$$dL_d/d\varphi = -[L_d^4/12B_0 D(y)][2(B_0/L_d^3)(\partial \tilde{Y}/\partial\varphi)_{L_d} + (15B_2/7)(a/b)^4(Y-2T)L_d \sin\varphi] \quad (1.77\text{a})$$

$$dL_d/d\varphi \approx -(B_2/21B_0)L_d^5(a/b)^4(1/12D)[45(Y-2T) + 4(147I_{12}-205I_{10}+54I_8)(2+y\ln y-2y^{1/2}) + 42yG_2(y)-75T(1)(2y+y\ln y-2y^{1/2})]\sin\varphi\,, \quad (1.77\text{b})$$

where (1.34c) defines $12D(y)\equiv 6T(y)-Y(y)$. The use of (1.77b) is made convenient by the development of an analytical approximation for

$$Q(y)\equiv 45Y(y)-90T(y)+42yG_2(y)-75T(1)(2y+y\ln y-2y^{1/2}) + 4(147I_{12}-205I_{10}+54I_8)(2+y\ln y-2y^{1/2}), \quad (1.78\text{a})$$

which must satisfy the conditions

$$Q(1) = -90T(1) \approx -66.6432441 \quad (1.78\text{b})$$

$$Q(0) = 8(147I_{12}-205I_{10}+54I_8) \approx -27.1266694 \quad (1.78\text{c})$$

$$Q'(1) = (15/2)[9T(0)-41T(1)] \approx -134.5360732\,. \quad (1.78\text{d})$$

Exact numerical evaluations [19, 36] of $T(y)$, $Y(y)$, and the shell-splitting function $Q/12D$ yield the functional values $Q(y)$ given in Table 4. Plotted on a graph (not shown here), these functional values indicate that $Q(y)$ varies only weakly with y for $y\lesssim 0.4$, but quite strongly for $y\gtrsim 0.7$, and that $Q(y)$ is *almost* a monotonic function. The empirical representation [66]

$$Q(y) \approx Q(0)+[2Q(1)-2Q(0)-(1/4)Q'(1)]y^4 + [Q(0)-Q(1)+(1/4)Q'(1)]y^8 \approx -27.12667-45.39913y^4+5.88256y^8 \quad (1.79)$$

provides numerical accuracy well within 1% over the entire range of y (see Table 4) in addition to satisfying the end-point ($y=0$ and $y=1$) requirements exactly. It is therefore proper to use (1.79) in combination with (1.28), (1.31), and (1.36) in the tracing of magnetospheric drift shells. No approximation for $G_1(y)$ is needed for this purpose, and so none has been developed.

Integration of (1.77b) with respect to φ leads directly to a lowest-order expression for tracing drift shells whose pitch-angle degeneracy is broken

Table 4. Exact and Approximate Values of $Q(y)$

θ_m	y	Exact Q	Approx. Q	$\Delta Q/Q$
0°	0.000000	−27.127	−27.127	0.0000
20°	0.028947	−27.085	−27.127	+0.0015
30°	0.093098	−27.090	−27.130	+0.0015
40°	0.206042	−27.118	−27.208	+0.0033
50°	0.367471	−27.777	−27.953	+0.0063
55°	0.462962	−29.051	−29.200	+0.0051
60°	0.564719	−31.645	−31.683	+0.0012
65°	0.668717	−36.026	−35.970	−0.0016
70°	0.769660	−42.509	−42.333	−0.0041
75°	0.860893	−50.378	−50.289	−0.0018
80°	0.934656	−58.313	−58.347	+0.0006
85°	0.983074	−64.323	−64.398	+0.0012
90°	1.000000	−66.643	−66.643	0.0000

by the day-night asymmetry of **B**. Two limiting cases of notable simplicity are recovered from (1.77b). For $y=1$ the drift trajectory is a path of constant B on the equatorial surface. For $y=0$ the drift shell follows field lines of equal arc length.

Numerical evaluation of (1.72) for the reasonable values $b=10a$ and $B_0=1.24B_1=1.48B_2=0.31$ gauss reveals that the right-hand side becomes negative on the day side ($\cos\varphi<0$) for $r\gtrsim 8a$. This behavior signals a bifurcation of the equatorial (minimum-B) surface as one approaches the magnetopause. In other words, dayside field lines for which L_d is sufficiently large ($\gtrsim 10$) satisfy $\partial B/\partial s=0$ and $\partial^2 B/\partial s^2>0$ at points symmetrically displaced in magnetic latitude from the equatorial plane of symmetry [5]. An "equatorially mirroring" particle (one with infinitesimal bounce amplitude) selects either the northern or southern branch of the equatorial (minimum-B) surface, depending upon the instantaneous value of its bounce phase φ_2 as the particle traverses the singular contour on which $\partial^2 B/\partial s^2=0$ in the plane of symmetry ($\theta=\pi/2$). Lowest-order expansions such as (1.68) apply only to drift shells on which each field line has a single minimum-B point.